International Journal of Research
Available at https://edupediapublications.org/journals
p-ISSN: 2348-6848
e-ISSN: 2348-795X
Volume 04 Issue 02
February 2017

Removal of Artifacts Based on Weighted Guided Filtering For Digital Video Quality Enhancement

N.Kavitha1; Sudhir Dakey2 & B.BhagyaSree3
[1, 2] Department of ECE, M.V.S.R Engineering College, Hyderabad.
[3] Department of ECE, Shadan College of Engineering and technology, Hyderabad.

Abstract

It is known that local filtering-based edge preserving smoothing techniques suffer from halo artifacts. Local filter cannot preserve sharp edges when compared to global filters. Such that, halo artifacts are usually produced when local filters adopt to smooth edges.In this paper, weighted guided image filter (WGIF) is proposed by incorporating an edge-aware weighting into an existing guided image filter (GIF) to address the problem. The WGIF is used to adopts both the advantages of global and local smoothing filters in the sense that: 1) the complexity of the WGIF is O(N) for an image with N pixels, which is same as the GIF and 2) the WGIF can avoid halo artifacts like the existing global smoothing filters. The WGIF is applied for single image detail enhancement, single image haze removal, and fusion of differently exposed images. Experimental results shows that the resultant image produces better visual quality by reducing/avoiding the halo artifacts to zero. The extension work is performed on videos, where this video consists of no. of frames. Each frame is converted into image. Every image is filtered by WGIF technique to avoid halo artifacts and to reduce the complexity. After then each image is again converted into frame and then video. The improved quality of video is shown in below results.

***KEYWORDS*:** Edge-preserving smoothing, weighted guided image filter, edge aware weighting, detail enhancement, haze removal.

1. INTRODUCTION

An important characteristic of edge-preserving regularization is that the computations involve the minimization of possibly nonconvex energy functionals. In many applications computation time is critical, so a deterministic strategy is preferable. Also, one has to face the problem of minimizing nonquadratic energy functionals or, equivalently, solving nonlinear simultaneous equations. In our second contribution of this paper, we show that, when the conditions for edge preservation are satisfied, it is possible to transform the nonquadratic energy into an augmented energy by introducing an auxiliary variable,*b*, whose role is twofold. First,*b* marks the location of discontinuities, and thus takes part in their preservation. Second, *b* makes the augmented energy functional become half-quadratic, i.e., quadratic with respect to the image variable when *b* is fixed. We also show that the augmented functional is convex with respect to when the image variable is fixed, and we give an exact expression for the minimum .

In human visual perception, edges provide an effective and expressive stimulation which is important for neural interpretation of a scene. In the fields of image processing and in many computational photography employ smoothing techniques which could preserve edges better [1],[4]. In smoothing process an image to be filtered is typically decomposed into two layers: a base layer composed by homogeneous regions with sharp edges and a detail layer formed by either noise, e.g., a random pattern with zero mean, or texture, e.g, a repeated pattern with usual arrangement. There are two types of edge-preserving image smoothing techniques: global filters such as the weighted least squares (WLS) [4] filter and local filters such as bilateral filter (BF) [9], trilateral filter, and their accelerated versions, as well as guided image filter (GIF) [14].Though the global optimization based filters frequently yield excellent quality, they have high computational cost. Comparing with the global optimization based filters, the local filters are generally simpler. However, the local filters cannot conserve sharp edges like the global optimization based filters.

Halo artifacts were usually produced by the local filters when they were adopted to smooth edges [14]. Major reason that the BF/GIF produces halo artifacts was both

International Journal of Research
Available at https://edupediapublications.org/journals
p-ISSN: 2348-6848
e-ISSN: 2348-795X
Volume 04 Issue 02
February 2017

spatial similarity parameter and range similarity parameter in the BF were fixed. But both the spatial similarity and the range similarity parameters of the BF could be [16] adaptive to the content of the image to be filtered. Unfortunately as pointed out, problem with adaptation of the parameters will destroy the 3D convolution form. We introduce in present paper, an edge-aware weighting technique and incorporated into the GIF to form a weighted GIF (WGIF). Local variance in 3×3 window of pixel in a guidance image is applied to calculate the edge-aware weighting. The local variance of a pixel is normalized by the local variance of all pixels in guidance image. The normalized weighting is then adopted to design the WGIF. As a result, halo artifacts can be avoided by using the WGIF. Similar to the GIF, the WGIF also avoids gradient reversal. In addition, the intricacy of the WGIF is O(N) for an image with N pixels which is the same as that of the GIF. These features allow many applications of the WGIF for single image detail enhancement, single image mist removal, and fusion of differently exposed images.

2. EDGE PRESERVING SMOOTHING TECHNIQUES

The task of edge-preserving smoothing is to crumble an image X into two parts as follows:

$$X(p) = \hat{J}(p) + e(p) \quad (1)$$

where $\hat{J}$ is a reconstructed image formed by uniform regions with sharp edges, e is noise or texture, and p(=(x,y)) is a position. J and e are called base layer and detail layer, respectively. One of edge-preserving smoothing techniques is based on local filtering. Bilateral filter (BF) is widely used due to its simplicity but suffer from "gradient reversal" [14] artifacts usually observed in detail enhancement of conventional LDR images. Then GIF was introduced to overcome this problem. In this GIF, a guidance image G was used which could be similar to the image X which is to be filtered.

$$\hat{J}(p) = ap'G(p) + bp', \ \forall p \in \Omega_\varsigma (p') \quad (2)$$

$\hat{J}$ is a linear transform of G in the window Ω_ς (p′).To determine the linear coefficients (ap′, bp′), a constraint is added to X and $\hat{J}$ as in Equation (1). The values of ap′ and bp′ are then obtained by minimizing a cost function E (ap′,bp′) which is defined as

$$E = \sum_{P \epsilon \Omega_\varsigma} \left[(ap'G(p) + bp' - X(p))^2 + \lambda ap'^2 \right] (3)$$

where λ is a regularization parameter.

Another type of edge-preserving smoothing techniques was based on global optimization. The Weighted Least Square filter was a typical example and it was derived by minimizing the following quadratic cost function:

$$E = \sum_{P=1}^{N} [(\hat{J}(p) - X(p))^2 + \lambda(p) \|\nabla \hat{J}(p)\|^2] \quad (4)$$

where N is the total number of pixels in an image.

$\nabla \hat{J}(p) = \left[\frac{\partial \hat{J}(p)}{\partial x}, \frac{\partial \hat{J}(p)}{\partial y} \right]^T$, and $\lambda(p) = [\lambda_x(p), \lambda_y(p)]^T$ is defined as

$$\lambda_x(p) = \frac{\lambda}{\left| \frac{\partial X(p)}{\partial x} \right| \gamma + \epsilon}; \ \lambda_y(p) = \frac{\lambda}{\left| \frac{\partial X(p)}{\partial y} \right| \gamma + \epsilon}$$

The two major differences between the WLS filter and the GIF

1) The GIF is based on local optimization while the WLS filter in based on global optimization. As such, the difficulty of the GIF is O(N) for an image with N number of pixels and the Weighted Least Square filter is more complicated than the GIF.

2) The value of λ is fixed in the GIF while it is adaptive to local gradients in the WLS filter. One possible problem for the GIF is halos which could be reduced by the WLS filter. The spatial varying image gradients aware weighting λx(p)and λy(p) are very important for the WLS filter to avoid halo artifacts.

Figure 1(a): Input image

Figure 1(b): Edge of input image

International Journal of Research
Available at https://edupediapublications.org/journals
p-ISSN: 2348-6848
e-ISSN: 2348-795X
Volume 04 Issue 02
February 2017

3. EXISTING METHODS

a) Bilateral Filter

The bilateral filter [9], [10] was perhaps the simplest which computed the filtering output at each pixel as the average of near-by pixels, weighted by the Gaussian of both range and spatial distance. The bilateral filter smooth's the image while preserving edges. Constraint of the bilateral filter was it endure from "gradient reversal" artifacts. The reason was that when a pixel (often on an edge) has few similar pixels around it, the Gaussian weighted average is unstable. Efficiency was another problem regarding the bilateral filter.

b) Non-average Filter

Edge-preserving filtering [4] could also be achieved by non average filters. The median filter [13] was a familiar edge-aware operator, and was a special case of local histogram filters. Histogram filters had O(N) time implementations in a way as the bilateral grid. The non-average filters were often computationally expensive.

c) Guided Image Filter

A general linear translation-variant filtering process, which involved a guidance image I [14], an filtering input image p, and an output image q. The filtering output at a pixel I was expressed as a weighted average:

$$qi = \sum_j Wij(I)pj \quad (4)$$

where i and j were pixel indexes. The filter kernel Wij was a function of the guidance image I and independent of p. This filter was linear with respect to p.

d) Adaptive Bilateral Filter

A content adaptive bilateral filter was proposed in gradient domain by taking the characteristics of the human visual systems into consideration. The proposed bilateral filter could be applied to extract fine details from a set of images simultaneously. Similar to the content adaptive bilateral filters the acceleration of the proposed filter could be an issue. Fortunately, the idea in might be borrowed to accelerate the proposed filter

e) Adaptive Guided Image Filter

An adaptive guided image filtering (AGF) [18] able to perform halo-free edge slope enhancement and noise reduction simultaneously. The intensity range domain of BLF and kernel function of GIF were similar in principle, because each of them takes the intensity value of center pixel p, local neighbors q and a smoothing parameter (σr in BLF, ε in GIF) in the computation process. This was based on the shifting technique of ABF, in which the offset ξp was added to the intensity value of center pixel pin the intensity range domain of BLF. The same strategy was applied to AGF - the offset is added to the intensity value. center pixel pin the kernel weights function of GIF.

4. PROPOSED METHOD

In this, an edge-aware weighting is first proposed and it is incorporated into the GIF to form the WGIF.

A) An Edge-Aware Weighting

Let *G* be a guidance image and be the variance of G in the 3 × 3 window,. An edge-aware weighting is defined by using local variances of 3 × 3 windows of all pixels as follows

$$\Gamma_{G(p')} = \frac{1}{N}\sum_{p=1}^{N}\frac{\sigma_{G,1}^2(p') + \varepsilon}{\sigma_{G,1}^2(p) + \varepsilon} \qquad (5)$$

Where ε is a small constant and its value is selected as $(0.001 \times L)^2$ while L is the dynamic range of the input image.

In addition, the weighting$\Gamma_G(p')$measures the importance of pixelp' with respect to the whole guidance image. Due to the box filter, the complexity of$\Gamma_G(p')$is O (N) for an image with N pixels. The value of $\Gamma_G(p')$ is usually larger than 1 if p' is at an edge and smaller than 1 if p' is in a smooth area. Clearly, larger weights are assigned to pixels at edges than those pixels in flat areas [17] by using the weight $\Gamma_G(p')$ in Equation (5).

By applying this edge-aware weighting, there might be blocking artifacts in final images. To prevent possible blocking artifacts from appearing in the final image, the value of $\Gamma_G(p')$ is smoothed by a Gaussian filter. The smoothed weights of all pixels in Fig. 1(a) are shown in Fig. 1(b). Clearly, larger weights are assigned to pixels at edges than those pixels in flat areas. The proposed weighting matches' one feature of human visual system, i.e., pixels at sharp edges are usually more efficient than those in flat areas.

B) The Proposed Filter

Same as the GIF, the key assumption of the WGIF is a local linear model between the guidance image G and the filtering output $\hat{f}$as in Equation (2). The model ensures that the output $\hat{Z}$ has an edge only if the guidance image G has an edge. The proposed weighting G(p) in Equation (5) is incorporated into the cost function E(a_p, b_p) in Equation (3). As such, the solution is obtained by minimizing the difference between the image to be filtered X and the filtering output $\hat{f}$ while maintaining the linear model (2),

International Journal of Research
Available at https://edupediapublications.org/journals
p-ISSN: 2348-6848
e-ISSN: 2348-795X
Volume 04 Issue 02
February 2017

i.e., by minimizing a cost function $E(a_{p'}, b_{p'})$which is defined as

$$E = \sum_{p\epsilon\Omega_{\zeta_1}(p')}\left[\left(a_{p'}G(p) + b_{p'} - X(p)\right)^2 + \frac{\lambda}{\Gamma_{G(p')}}a_{p'}^2\right] \quad (6)$$

The optimal values of $a_{p'}$ and $b_{p'}$ are computed as

$$a_{p'} = \frac{\mu_{G\odot X,\zeta_1}(p') - \mu_{G,\zeta_1}(p')\mu_{X,\zeta_1}(p')}{\sigma^2_{G,\zeta_1}(p') + \frac{\lambda}{\Gamma_{G(p')}}} \quad (7)$$

$$b_{p'} = \mu_{X,\zeta_1}(p') - a_{p'}\mu_{G,\zeta_1}(p') \quad (8)$$

where $\odot$ is the element-by-element product of two matrices.$\mu_{G\odot X,\zeta_1}(p'), \mu_{G,\zeta_1}(p')$ and $\mu_{X,\zeta_1}(p')$are the mean values of G$\odot$ X, G and X, respectively.

The final value of Z^ (p) is given as follows:

$$\hat{Z}(p) = \bar{a}_p G(p) + \bar{b}_p \quad (9)$$

Where $\bar{a}_p$ and $\bar{b}_p$are the mean values of and in the window computed as

$$\bar{a}_p = \frac{1}{|\Omega_{\zeta_1}(p)|}\sum_{p'\epsilon\Omega_{\zeta_1}(p)} a_{p'}\ ; \bar{b}_p = \frac{1}{|\Omega_{\zeta_1}(p)|}\sum_{p'\epsilon\Omega_{\zeta_1}(p)} b_{p'} \quad (10)$$

And $|\Omega_{\zeta_1}(p')|$is the cardinality of $\Omega_{\zeta_1}(p')$.

For easy analysis, the images X and G are assumed to be the same. Consider the case that the pixel p' is at an edge. The value of $\Gamma_X(p')$ is usually much larger than 1.$a_{p'}$ in the WGIF is closer to 1 than $a_{p'}$in the GIF. This implies that sharp edges are preserved better by the WGIF than the GIF. As shown in Fig. 3, edges are indeed preserved much better by the WGIF. In addition, the complexity of the WGIF is O(N) for an image with N pixels which is the same as that of the GIF. Edges are also preserved well by the ABF while the complexity of the ABF is an issue

C.Single Image/Frame Haze Removal

Images of outdoor scenes could be degraded by haze, fog, and smoke in the atmosphere. The degraded images lose the contrast and color fidelity. Haze removal is thus highly desired in both computational photography and computer vision applications. The model adopted to describe the formulation of a haze image is given as [7]

$$X_c(p) = \hat{Z}_c(p)t(p) + A_c\left(1 - t(p)\right) \quad (10)$$

When the atmosphere is homogenous, the transmission t(p) can be expressed as:

$$t(p) = e^{-ad(p)} \quad (11)$$

Let $\phi_c(\cdot)$be a minimal operation along the color channel $\{r, g, b\}$ and it is defined as

$$A_{min} = \phi_c(A_c) = \min\{A_r, A_g, A_b\} \quad (12)$$

$$X_{min}(p) = \phi_c\left(X_c(p)\right) = \min\{X_r(p), X_g(p), X_b(p)\} \quad (13)$$

$$\hat{Z}_{min}(p) = \phi_c\left(\hat{Z}_c(p)\right) = \min\{\hat{Z}_r(p), \hat{Z}_g(p), \hat{Z}_b(p)\} \quad (14)$$

it can be derived from the haze image model in Equation (15) that

$$X_{min}(p) = \hat{Z}_{min}(p)t(p) + A_{min}\left(1 - t(p)\right) \quad (15)$$

Let $\psi_{\zeta_2}(\cdot)$be a minimal operation in the neighborhood $\psi_{\zeta_2}(p)$and it is defined as

$$\psi_{\zeta_2}\left(z(p)\right) = \min_{p'\epsilon\Omega_{\zeta_2}(p)}\{z(p')\} \quad (16)$$

It is shown that the complexity of $\psi_{\zeta_2}(\cdot)$ is O(N) for an image with N pixels. The dark channel is defined as

$$J^{\hat{Z}}_{dark}(p) = \phi_c\left(\psi_{\zeta_2}\left(\hat{Z}_c(p)\right)\right) \quad (17)$$

where the value of ζ_2 is 7. Even though the complexity of $\psi_{\zeta_2}(\cdot)$is O(N) for an image with N pixels, three minimal operations $\psi_{\zeta_2}(\cdot)$and one minimal operation $\Phi_c(\cdot)$are required to compute $J^{\hat{Z}}_{dark}(p)$ for the pixel p.simplified dark channel is defined as

$$\hat{J}^{\hat{Z}}_{dark}(p) = \psi_{\zeta_2}\left(\phi_c\left(\hat{Z}_c(p)\right)\right) \quad (18)$$

The value of $t(p)$ is assumed to be constant in the neighborhood$\Omega_{\zeta_1}(p')$. It can be derived from Equation (20) that

$$\hat{J}^{X}_{dark}(p) = \hat{J}^{\hat{Z}}_{dark}(p)t(p) + A_{min}\left(1 - t(p)\right) \quad (19)$$

Since $\hat{J}^{\hat{Z}}_{dark}(p) \approx 0$, the value of $t(p)$ can be initially estimated as

$$t(p) = 1 - \frac{\hat{J}^{X}_{dark}(p)}{A_{min}} \quad (20)$$

It is worth noting that the initial value of t(p) is given as

$$t(p) = 1 - \phi_c\left(\psi_{\zeta_2}\left(\frac{\hat{Z}_c(p)}{A_c}\right)\right) \quad (21)$$

The initial value of$t(p)$is then computed as

$$t(p) = 1 - \frac{31}{32}\frac{\hat{J}^{X}_{dark}(p)}{A_{min}} \quad (22)$$

The value of λ is set to 1/1000 and the value of ζ_1 to 60. The value of the transmission map$t(p)$ is further adjusted as

$$t(p) = t^{1+\varsigma}(p) \quad (23)$$

where the value of ς is adaptive to the haze level of the input image. Its value is 0/0.03125/0.0625 if the input image is with light/normal/heavy haze.

Finally, the scene radiance $\hat{Z}(p)$ is recovered by

International Journal of Research
Available at https://edupediapublications.org/journals
p-ISSN: 2348-6848
e-ISSN: 2348-795X
Volume 04 Issue 02
February 2017

$$\hat{Z}_c(p) = \frac{X_c(p)-A_c}{t(p)} + A_c \; ; c\epsilon\{r,g,b\} \qquad (24)$$

Equation (29) is equivalent to

$$\hat{Z}_c(p) = X_c(p) + \left(\frac{1}{t(p)} - 1\right)(X_c(p) - A_c) \qquad (25)$$

Since the color of the sky is usually very similar to the atmospheric light Ac in a haze image, it can be shown that

$$\frac{\hat{J}^X_{dark}(p)}{A_{min}} \to 1, and, \frac{1}{t(p)} - 1 \to 31 \qquad (26)$$

5. SIMULATION RESULTS

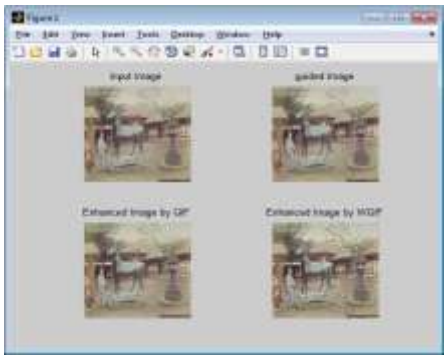

(c) Enhanced image by GIF (d) Enhanced image by WGIF

Analysis 2: In the above figure first is the input image which is to be analyzed and the second is guided image which is not but a filtering technique which preserves the edges of an image, the third one is GIF image with less preserving edges. The last one is proposed method which shows image with zero artifacts.

Analysis 3: The above applies weights on the edges of an image to preserve edges of an image occurred by the filtering technique.

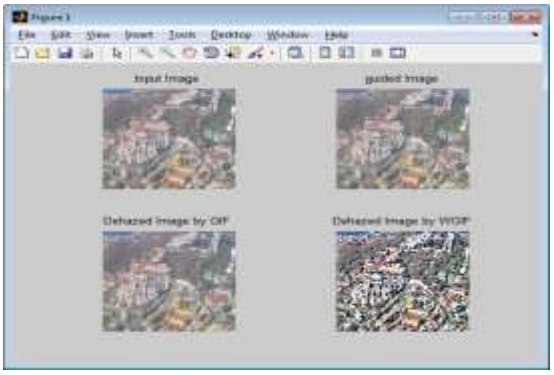

Figure 4: (a) Input image (b) Guided image (c) Dehazed image by GIF (d) Dehazed image by WGIF

Analysis 4: The above figure is used to dehaze the image from smoke etc as shown by applying different techniques.

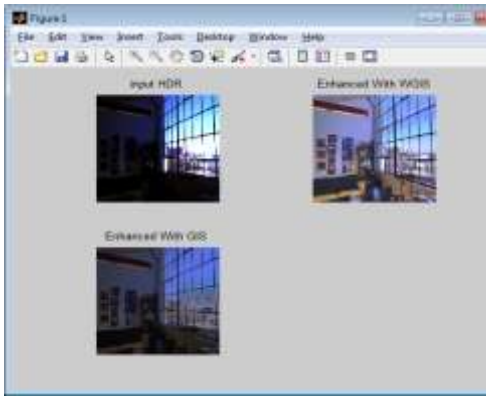

with WGIS (c) Enhanced with GIS

Analysis 5: This figure is used to show the enhancement of an image with improved picture quality by different edge preserving techniques.

6. EXTENSION

Proposed method has been performed improved image quality on images. For extension, we are performing on videos. Compare to images the complexity for videos is more because a video consist of no. of frames. As the no. of frames increases the reduction of complexity is also gets increased. But, avoiding all these complexities every frame is avoiding halo artifacts and preserves edges. At last all these frames converted into video.

International Journal of Research
Available at https://edupediapublications.org/journals
p-ISSN: 2348-6848
e-ISSN: 2348-795X
Volume 04 Issue 02
February 2017

Figure 6: Input video

Analysis 6: The above figure shows the input video which consist of some set of frames.

Figure 7: GI Video

Analysis 7: The above figure shows GI video which has better results than the input video .

Figure 8: GIF Video

Analysis 8: The above figure shows GIF video which has better quality than the GI video .

Figure 9: WGIF Video

Analysis 9: The above figure shows WGIF video which has better image quality than the GIF video .

Figure 9: Weights on WGIF Video

Analysis 9: The above figure shows weights applied on WGIF video to preserves edges.

7. CONCLUSION

This method is introduced by incorporating an edge-aware weighted into an existing guided image filter (GIF). It has two advantages of both global and local smoothening filter in the sense-(1) Its complexity is 0,(2)Avoid halo artifacts The output of WGIF results in better visual quality and avoid halo artifacts. , it has many applications in the fields of computational photography and image processing. Particularly, it is applied to study single image detail enhancement, single image haze removal, and fusion of differently exposed images. Experimental results show that the resultant algorithms can produce images with excellent visual quality as those of global filters, and at the same time the running times of the proposed algorithms are comparable to the GIF based algorithms. It is noting that the WGIF can also be adopted to design a fast local tone mapping algorithm for high dynamic range images, joint up

sampling, flash/no-flash de-noising, and etc. In addition, similar idea can be used to improve the anisotropic diffusion, Poisson image editing, etc. All these research problems will be studied in our future research.

REFERENCES

[1] P. Charbonnier, L. Blanc-Feraud, G. Aubert, and M. Barlaud, "Deterministic edge-preserving regularization in computed imaging," IEEE Trans. Image Process., vol. 6, no. 2, pp. 298–311, Feb. 1997.

[2] L. I. Rudin, S. Osher, and E. Fatemi, "Nonlinear total variation based noise removal algorithms," Phys. D, Nonlinear Phenomena, vol. 60, nos. 1–4, pp. 259–268, Nov. 1992.

[3] Z. G. Li, J. H. Zheng, and S. Rahardja, "Detail-enhanced exposure fusion," IEEE Trans. Image Process., vol. 21, no. 11, pp. 4672–4676, Nov. 2012.

[4] Z. Farbman, R. Fattal, D. Lischinski, and R. Szeliski, "Edge-preserving decompositions for multi-scale tone and detail manipulation," ACM Trans. Graph., vol. 27, no. 3, pp. 249–256, Aug. 2008.

[5] R. Fattal, M. Agrawala, and S. Rusinkiewicz, "Multiscale shape and detail enhancement from multi-light image collections," ACM Trans. Graph., vol. 26, no. 3, pp. 51:1–51:10, Aug. 2007.

[6] P. Pérez, M. Gangnet, and A. Blake, "Poisson image editing," ACM Trans. Graph., vol. 22, no. 3, pp. 313–318, Aug. 2003.

[7] K. He, J. Sun, and X. Tang, "Single image haze removal using dark channel prior," IEEE Trans. attern Anal. Mach. Intell., vol. 33, no. 12, pp. 2341–2353, Dec. 2011.

[8] L. Xu, C. W. Lu, Y. Xu, and J. Jia, "Image smoothing via L0 gradient minimization," ACM Trans. Graph., vol. 30, no. 6, Dec. 2011, Art. ID 174.

[9] C. Tomasi and R. Manduchi, "Bilateral filtering for gray and color images," in Proc. IEEE Int. Conf. Comput. Vis., Jan. 1998, pp. 836–846.

[10] Z. Li, J. Zheng, Z. Zhu, S. Wu, and S. Rahardja, "A bilateral filter in gradient domain," in Proc. Int. Conf. Acoust., Speech Signal Process., Mar. 2012, pp. 1113–1116.

[11] P. Choudhury and J. Tumblin, "The trilateral filter for high contrast images and meshes," in Proc. Eurograph. Symp. Rendering, pp. 186–196, 2003.

[12] F. Durand and J. Dorsey, "Fast bilateral filtering for the display of highdynamic-range images," ACM Trans. Graph., vol. 21, no. 3, pp. 257–266, Aug. 2002.

[13] J. Chen, S. Paris, and F. Durand, "Real-time edge-aware image processing with the bilateral grid," ACM Trans. Graph., vol. 26, no. 3, pp. 103–111, Aug. 2007.

[14] K. He, J. Sun, and X. Tang, "Guided image filtering," IEEE Trans. Pattern Anal. Mach. Intell., vol. 35, no. 6, pp. 1397–1409, Jun. 2013.

[15] B. Y. Zhang and J. P. Allebach, "Adaptive bilateral filter for sharpness enhancement and noise removal," IEEE Trans. Image Process., vol. 17, no. 5, pp.664–678,May2008.